Nucleation theory of overdamped soliton motion

M. Büttiker and R. Landauer
IBM Thomas J. Watson Research Center, Yorktown Heights, New York 10598
(Received 5 September 1980)

We consider a ring of tightly torsion-coupled, overdamped pendulums subject to an external torque and coupled to a thermal reservoir. At low temperatures the dynamics of this system, over a wide range of forces, is governed by thermally activated kink-antikink pairs, their subsequent separation through the external force, and eventual recombination by collision with other kinks. We calculate the thermal activation rate of kink-antikink pairs using an approach first developed by Brinkman. This theory requires a detailed investigation of the multidimensional saddle, which has to be crossed, if the system is to make a thermally activated transition. The propagation velocity of the driven kinks is calculated. We use these results to derive the mean angular pendulum velocity as a function of the applied torque. Comparison is made with earlier work.

I. INTRODUCTION

In this paper we consider the thermal activation of large-amplitude excitations of a chain of particles separated from each other in the x direction, and subject to displacement in an orthogonal direction θ. The particles are in a periodic potential $V_0(1-\cos\theta)$ and under the action of an external driving force potential $-F\theta$. We assume that the coupling between two adjacent particles is strong enough, so that neighboring particles remain close to each other in the θ direction. If the motion of the particles is heavily damped, the equation of motion for this system is

$$\gamma\frac{\partial\theta}{\partial t}=-V_0\sin\theta+F+\kappa\frac{\partial^2\theta}{\partial x^2}+\zeta\,, \tag{1.1}$$

where γ is the damping constant and ζ is a thermal random force with $\langle\zeta\rangle=0$ and strength

$$\langle\zeta(x,t)\zeta(x',t')\rangle=2\gamma kT\delta(t-t')\delta(x-x')\,. \tag{1.2}$$

The underdamped limit of Eq. (1.1), including the inertial terms omitted here, has been studied extensively in dislocation theory.[1] A typical low-temperature configuration of the displacement field $\theta(x,t)$ is shown in Fig. 1. Following the dislocation literature[1] we call a local maximum of the potential $V_0(1-\cos\theta)-F\theta$ a Peierls hill, and a local minimum a Peierls valley. The Peierls valleys exist only for $|F|<V_0$. This is the field range in which we are interested. At low temperatures, transitions over Peierls hills are far apart, and most of the chain will lie in the Peierls valleys. Transitions connecting the segments of the chain lying in different Peierls valleys will be called kinks, if their first spatial derivative is positive, and antikinks, if their first spatial derivative is negative. One can make a further distinction between geometrical and thermal kinks.[1] If the field $\theta(x,t)$ is pinned at $x=0$ and L in different Peierls valleys the chain must necessarily span the Peierls hills between $\theta(0)$ and $\theta(L)$ and a number of kinks must be present even at zero temperature. The number of these geometric kinks is determined solely by the geometric arrangement of the pinning points. On the other hand, if the pinning points $\theta(0)$ and $\theta(L)$ are in the same Peierls valley or if one assumes periodic boundary conditions $\theta(x,t)=\theta(x+L,t)$, as we will in this paper, kinks are only present as a result of thermal activation. These thermal kinks are created in pairs involving a kink and an antikink, "... analogous to the formation of electron-hole pairs in intrinsic semiconductors.[1]" In contrast to the geometrical kinks, the density of the thermal kinks depends strongly on the temperature, as shown in Ref. 1.

The aim of this paper is to present a detailed calculation of the nucleation rate of kink-antikink pairs in the overdamped and forced sine-Gordon chain. Our results have been reported in Ref. 2. In connection with the theory of kinks in dislocations, repeated attempts have been made to calculate this important quantity. The work in this field has been reviewed and extended in Ref. 1, and we

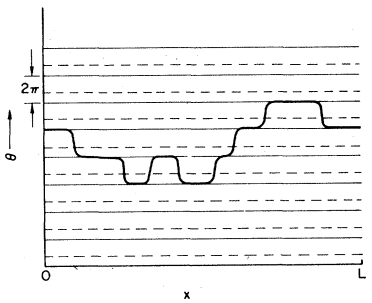

FIG. 1. Typical low-temperature configuration of the displacement field $\theta(x,t)$ at a given instant of time. Long segments of the chain lying in a Peierls valley (thin solid lines) are connected by kinks and antikinks which span the Peierls hills (thin broken lines).

refer to this paper for further references.

The problem which has to be solved is the following. Consider a length of the chain lying initially in a Peierls valley. A thermal fluctuation can throw a piece of the chain into the next valley, favored by the applied force F. If the segment is too small, then the attraction between the newly formed kink and antikink outweighs the driving force F and the incipient nucleus collapses. If, however, the segment is long enough, then the driving force F predominates and the nucleus expands. Thus there is a critical nucleus, i.e., a configuration belonging to a saddle point of the energy surface. This saddle point has to be crossed for the thermal activation of a kink-antikink pair. Reference 1 attacked this problem by two approaches: One was based on Kramers's theory[3] for the rate of thermally activated transitions over a one-dimensional barrier, thus ignoring the many-dimensional nature of the saddle point. The other approach followed the theory outlined by Vineyard,[4] who takes into account the many degrees of freedom, but assumes that the transition rate can be found from an analysis of the barrier-crossing rate in a thermal equilibrium problem. This overestimates the transition rate. Brinkman,[5] Landauer and Swanson,[6] and Langer,[7] (hereafter abbreviated as BLSL), were able to combine the Kramers and Vineyard approaches and to formulate a theory treating the thermally activated crossing over a many-dimensional saddle point. We will apply the BLSL approach to the nucleation rate of kink-antikink pairs.

In recent years the statistical mechanics of solitons has found new interest,[8,9] unrelated to previous results in the theory of kinks in dislocations. This development was stimulated by an application of the transfer-operator technique[10] to systems exhibiting solitons.[11] This transfer-operator technique combined with a low-order Bogoliubov-Green-Kirkwood-Yvon (BBGKY) hierachy approximation[12-14] has been used to find the average rate at which θ advances with time. We will evaluate the same quantity and compare our results with Refs. 12–14 and with computer simulations of the sine-Gordon chain.[15] In contrast to the approach via the BBGKY hierachy the BLSL theory provides a nonperturbative answer.

Our paper is organized in the following way. In Sec. II we discuss the critical nucleus, i.e., the saddle-point configuration. In Sec. III, we investigate the energy surface near the saddle. In Sec. IV, we use the BLSL approach to calculate the rate of formation of kink-antikink pairs. In Sec. V, we evaluate the drift velocity of the kinks in the presence of an applied field, and investigate the steady-state motion of the chain. In Sec. VI, we discuss our results and compare them with previous work.

II. ACTIVATION ENERGY BARRIER FOR KINK-ANTIKINK PAIRS

The variation of the energy functional

$$E(\theta)=\int dx\left[V+\frac{\kappa}{2}\left(\frac{\partial\theta}{\partial x}\right)^2\right], \tag{2.1}$$

governs the deterministic time evolution of the displacement field $\theta(x,t)$:

$$\gamma\frac{\partial\theta}{\partial t}=-\frac{\delta E(\theta)}{\delta\theta}\,. \tag{2.2}$$

Here,

$$V=V_0(1-\cos\theta)-F\theta\,, \tag{2.3}$$

includes the Peierls energy $V_0(1-\cos\theta)$ and the external driving potential $-F\theta$. The potential V has stationary points for $|F|\leq V_0$ given by

$$\theta_{s,n}=2n\pi+\arcsin(F/V_0)\,, \tag{2.4a}$$

$$\theta_{u,n}=(2n+1)\pi+\arcsin(F/V_0)\,. \tag{2.4b}$$

In the states $\theta_{s,n}$ the chain lies uniformly in one of the Peierls valleys (potential minima) and is stable (index s) against small perturbations. In the states $\theta_{u,n}$ the chain lies uniformly along a Peierls hill and is unstable (index u) against small perturbations. The energy density of the chain lying in a Peierls valley and on a Peierls hill, respectively, are given by

$$V_{s,n}=E(\theta_{s,n})/L=V_0(1-\cos\theta_{s,n})-F\theta_{s,n}\,, \tag{2.5a}$$

$$V_{u,n}=E(\theta_{u,n})/L=V_0(1-\cos\theta_{u,n})-F\theta_{u,n}\,. \tag{2.5b}$$

The chain in the Peierls valley $n+1$ has a potential energy which is $2\pi FL$ lower than a chain in the valley n. The state $\theta_{s,n}$ is only a metastable state. The fluctuation assisted transition of the chain from one valley to the next one will be most likely to occur through a time sequence of configurations requiring the minimum intermediate elevation in energy. Therefore, we have to search for a saddle point in the energy surface $E(\theta)$ through which the chain configuration can pass.[5-7,16,17]
A saddle point requires the following conditions:

(1) It is a local extremum of the energy surface. The first variation of the energy must vanish at the point $\theta_N(x)$ in function space $\delta E/\delta\theta\big|_{\theta=\theta_N}=0$. The saddle-point configuration $\theta_N(x)$ (critical nucleus) is, therefore, a stationary (time-independent) solution of the equation of motion (2.2).

(2) The energy $E(\theta)$ increases or remains constant in all but one direction as one moves away from $E(\theta_N)$, i.e., the second variation $\delta^2E/\delta\theta^2\big|_{\theta=\theta_N}$ is nonnegative in all but one direction.

The stationary points of the energy surface are given by the solutions of

$$\frac{\delta E(\theta)}{\delta\theta} = -V_0 \sin\theta + F + \kappa d^2\theta/dx^2 = 0 . \tag{2.6}$$

Multiplying Eq. (2.6) with $d\theta/dx$ and integrating yields

$$\frac{\kappa}{2}\left(\frac{d\theta}{dx}\right)^2 - V = U_0 , \tag{2.7}$$

where U_0 is an integration constant. The total energy of a stationary solution is found by inserting Eq. (2.7) into Eq. (2.1) which gives

$$E(\theta) = \int dx \left[\kappa\left(\frac{d\theta}{dx}\right)^2 - U_0\right]. \tag{2.8}$$

It is convenient to calculate the excess energy of the nonuniform configurations

$$\Delta E(\theta) = E(\theta) - E(\theta_s) = \int dx \left[\kappa\left(\frac{d\theta}{dx}\right)^2 - U_0 - V_s\right], \tag{2.9}$$

with respect to the energy $E(\theta_s)$ of a uniform stationary state defined in Eqs. (2.4a) and (2.5a). For simplicity we drop from now on the index n on $\theta_{s,n}$, $V_{s,n}$ and $V_{u,n}$.

Equation (2.6) describes the motion of a classical particle with mass $m = \kappa$, time $t = x$, in a potential $U = -V$, V given by Eq. (2.3). Equation (2.7) states the law of conservation of energy for this motion. The potential U is shown in Fig. 2. For $-V_u < U_0 < -V_s$, with V_u and V_s given by Eqs. (2.5a) and (2.5b), the particle undergoes anharmonic oscillations[18] around θ_u. For $U_0 > -V_s$ a particle coming from the left eventually reaches a turning point and departs to infinity. The critical nucleus will be a configuration which deviates only in a localized region from the uniform state θ_s. It is, therefore, a solution with initial energy $U = -V_s$. This energy yields a trajectory which describes the exponential departure of the particle from the local maximum $U = -V_s$, followed by the motion to the right until the turning point at $\theta = \theta_s + \Delta\theta_m$ is reached. The particle then again returns asymptotically to the local maximum at θ_s. The corresponding stationary solution of Eq. (2.6) is the saddle-point configuration or critical nucleus $\theta_N(x)$ (Fig. 3). This configuration departs from the stationary uniform state θ_s, at $x = \pm\infty$, with an exponential decay length

$$\xi(F) = (\kappa/V_0)^{1/2}(\cos\theta_s)^{-1/2} = (\kappa/V_0)^{1/2}[1 - (F/V_0)^2]^{-1/4} . \tag{2.10}$$

$\xi(F)$ increases monotonically with F from its equilibrium value $\xi_0 = \xi(0) = (\kappa/V_0)^{1/2}$ and diverges as F approaches V_0. The excess energy of the critical nucleus is given by

$$\Delta E_N = \Delta E(\theta_N) = \int \kappa\left(\frac{d\theta_N}{dx}\right)^2 dx , \tag{2.11}$$

as follows from Eq. (2.9) with $U_0 = -V_s$.

In special cases, we can derive an analytical expression for the saddle-point configuration $\theta_N(x)$. For convenience, we introduce the deviation of the displacement $\Delta\theta_N(x) = \theta_N(x) - \theta_s$ away from the stationary uniform state θ_s. Equation (2.6) becomes

$$\frac{1}{2}\xi^2\left(\frac{d\Delta\theta_N}{dx}\right)^2 = \tan\theta_s(\sin\Delta\theta_N - \Delta\theta_N) + (1 - \cos\Delta\theta_N) . \tag{2.12}$$

Equation (2.12) can be integrated by separation of variables, so that formally the saddle-point configuration is given by

$$\int \frac{d\Delta\theta_N}{[\tan\theta_s(\sin\Delta\theta_N - \Delta\theta_N) + (1 - \cos\Delta\theta_N)]^{1/2}} = \pm\sqrt{2}\left(\frac{x}{\xi}\right). \tag{2.13}$$

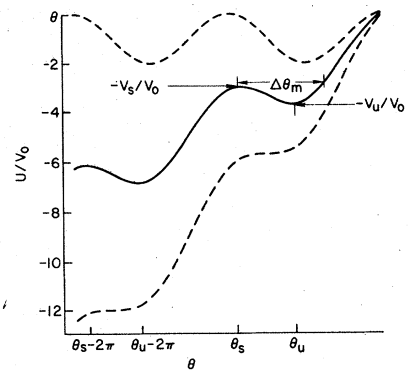

FIG. 2. Potential $U = -V = -V_0(1 - \cos\theta) + F\theta$ for $F/V_0 = 0.5$ (solid line) and the limiting values $F/V_0 = 0$ and $F/V_0 = 1$ (broken lines). For $|F| < V_0$ a particle with energy U_0 in the interval $(-V_u, -V_s)$ exhibits nonlinear oscillations around θ_u. The critical nucleus corresponds to the trajectory of a particle started at θ_s with energy $U_0 = -V_s$. The maximum deviation from θ_s in this trajectory is $\Delta\theta_m$.

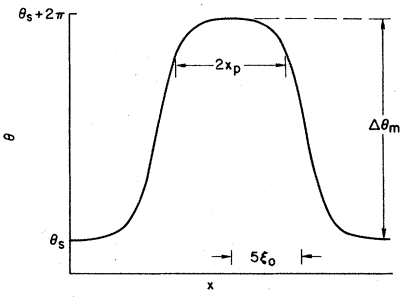

FIG. 3. Large-amplitude nucleus (LAN) for $F/V_0 = 10^{-4}$. The flat top of the LAN has a width $2x_p \propto \xi_0 \log(4\pi F/V_0)$, where $\xi_0 = (\kappa/V_0)^{1/2}$.

For F close to V_0 we can expand the right-hand side (rhs) of Eq. (2.12), or the denominator of Eq. (2.13), in powers of $\Delta\theta_N$. Such an expansion is possible because in this limit θ_s and θ_u come close to each other and the maximal excursion $\Delta\theta_m$ of the saddle-point configuration is small compared to 2π and is of the order of $\theta_u - \theta_s$. Neglecting powers higher than the third order in $\Delta\theta_N$, we find a small-amplitude nucleus, hereafter called (Ref. 2) SAN,

$$\theta_{\mathrm{SAN}}(x) = \theta_s + \Delta\theta_m \frac{1}{\cosh^2(x/2\xi)}, \tag{2.14}$$

with amplitude $\Delta\theta_m = 3\sqrt{2}[(V_0 - F)/V_0]^{1/2}$. This amplitude decreases to zero at $F = V_0$ and the width $4\xi = 4\xi_0[2(V_0 - F)/V_0]^{-1/4}$ diverges as F approaches V_0.

We will show that for small fields the critical nucleus consists of a kink,

$$\Delta\theta_K = 4\arctan[\exp(x/\xi_0)], \tag{2.15}$$

and an antikink separated by a distance $\xi_0 \log(V_0/F)$, with a maximum displacement $\Delta\theta_m = 2\pi - (4\pi F/V_0)^{1/2}$. The kink and antikink solutions are found from Eq. (2.13) at $F = 0$. The distance between the kink and antikink is determined by the flat top of this large-amplitude nucleus (LAN). To find the shape of the LAN near the maximum displacement $\Delta\theta_m$, we expand in $\phi = \Delta\theta_m - \Delta\theta$. For small fields Eq. (2.12) yields

$$\frac{1}{2}\xi_0^2\left(\frac{d\phi}{dx}\right)^2 = \left(\frac{4\pi F}{V_0}\right)^{1/2}\phi + \tfrac{1}{2}\phi^2. \tag{2.16}$$

At $F = 0$ this equation describes the exponential tails of the kink and antikink solutions. For $F \neq 0$ the first term describes the behavior near the turning point $\theta = \theta_s + \Delta\theta_m$ in Fig. 2. Requiring $\phi = 0$ at $x = 0$ (i.e., $\Delta\theta(0) = \Delta\theta_m$), we find from Eq. (2.16),

$$x = \xi_0 \log\{2[(\phi/\phi_0) + (\phi/\phi_0)^2]^{1/2} + 2(\phi/\phi_0) + 1\}, \tag{2.17}$$

where $\phi_0 = 2(4\pi F/V_0)^{1/2}$ is the angle at which the linear and quadratic term of the right-hand side of Eq. (2.16) are of the same magnitude. For $\phi > \phi_0$ only the quadratic term, which governs the exponential behavior of the kink solutions, is important. To find the width of the flat top of the LAN, we have to extend the above integration to an angle $\phi_p \gg \phi_0$, but keeping $\phi_p \ll 2\pi$, so that the quadratic term in Eq. (2.16) is still accurate. This can be done because ϕ_0 is very small for very small F. The flat top of the LAN, therefore, has an extension $2x_p$ with x_p given by

$$x_p \cong \xi_0(\log 4\phi_p - \log\phi_0) \cong -(\xi_0/2)\log(4\pi F/V_0). \tag{2.18}$$

Because $\phi_p \gg \phi_0$ the contribution of ϕ_p to x_p can be neglected.

With these results, we can now calculate the energy barrier, ΔE_N defined by Eq. (2.11), required for crossing the saddle point. With Eq. (2.14), we find in the limit of the SAN[2],

$$\Delta E_N(F) = (3/5)E_0[2(V_0 - F)/V_0]^{5/4}. \tag{2.19}$$

Because the local minima of the potential V [Eq. (2.3)] disappear at $F = V_0$, the activation energy $\Delta E_N(F)$ also goes to zero at $F = V_0$. For the LAN we can find $\Delta E_N(F)$ in the following way. As we approach equilibrium the activation energy barrier for a kink-antikink pair approaches the sum of the rest energy of a kink and an antikink. With Eqs. (2.15) and (2.18) we find,

$$\Delta E_N(0) = 2E_0, \quad E_0 = 8(\kappa V_0)^{1/2}. \tag{2.20}$$

The energy is stationary at θ_N with respect to small changes in the configuration. Therefore, the energy changes to first order in dF, only because the potential V which the saddle-point configuration θ_N sees changes. For very small F the important contribution comes from the change of the flat top part of the configuration θ_N near $\Delta\theta = \Delta\theta_m$. Thus by considering Eq. (2.1), we find

$$d\Delta E_N = -dF\,W, \tag{2.21}$$

where

$$W = \int_{-\infty}^{+\infty} \theta_N(x)dx \cong 2\pi(2x_p). \tag{2.22}$$

In Eqs. (2.21) and (2.22), we have used the fact that the largest part of the LAN is the flat top whose width is given by Eq. (2.18). The energy of the LAN is found by integrating Eq. (2.21), with the use of Eq. (2.18) and Eq. (2.20). This yields

$$\Delta E_N(F) = 2E_0 + 2\pi\xi_0 F\log(4\pi F/V_0). \tag{2.23}$$

To find $\Delta E_N(F)$ in the whole range $0 \leq F \leq V_0$, we have integrated Eq. (2.11) numerically. The result is shown in Fig. 4. The resolution of the numerical integration is too coarse to show the singularity in the derivative at $F = 0$ predicted by Eq. (2.23).

III. THE SADDLE

In the previous section, we discussed the stationary solutions $\Delta\theta(x) = \theta(x) - \theta_s$ which correspond to local extrema of the energy surface [Eq. (2.1)]. We will now investigate the stability of these solutions. We add small perturbations $\delta\theta(x,t)$ to $\theta(x)$ and linearize the time-evolution equation (2.2) with respect to these perturbations. Because the unperturbed solutions $\theta(x)$ are time independent, the perturbations can be assumed to have the form $\delta\theta(x,t) = \delta\theta_\lambda(x)\exp(-\lambda t)$. This leads

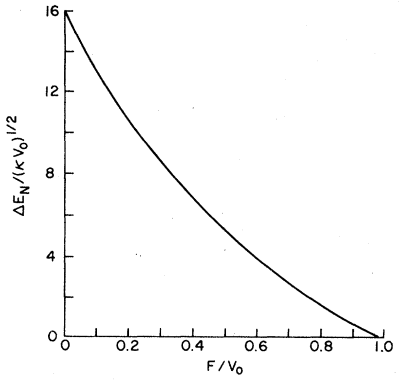

FIG. 4. Activation energy barrier as a function of the field. The curve shown is universal, i.e., independent of γ, V_0, κ.

to the eigenvalue problem

$$L(\theta(x))\delta\theta_\lambda(x) = (\lambda/\Gamma)\delta\theta_\lambda(x)\,, \tag{3.1}$$

where the linear operator $L(\theta(x))$ is given by

$$L(\theta(x)) = -\xi^2 d^2/dx^2 + R(\theta(x))\,. \tag{3.2a}$$

The potential

$$R(\theta(x)) = [\cos\Delta\theta(x) - \tan\theta_s \sin\Delta\theta(x)] \tag{3.2b}$$

of the Schrödinger operator, Eq. (3.2a), is generated by the stationary solution $\Delta\theta(x) = \theta(x) - \theta_s$. Here $\Gamma = V_0\cos\theta_s/\gamma$ and θ_s and ξ^2 are determined by Eqs. (2.4a) and (2.10), respectively. The operator L is self-adjoint in the scalar product $\langle\phi|\psi\rangle = a^{-1}\int dx\, \phi^*(x)\psi(x)$. The spacing a between neighboring pendulums has been taken into the definition of the scalar product to make it dimensionless. Because L is self-adjoint, it has a complete set of eigenfunctions ψ_n which are normalized such that $\langle\psi_n|\psi_m\rangle = \delta_{n,m}$. We can now expand the perturbation $\delta\theta(x,t)$ in terms of the eigenfunctions

$$\delta\theta(x,t) = \sum_m \eta_m|\psi_m\rangle, \quad \eta_m = \langle\psi_m|\delta\theta\rangle\,, \tag{3.3}$$

and obtain for the energy in the neighborhood of a local extremum

$$E(\theta(x)+\delta\theta(x)) = E(\theta(x)) + \frac{a\gamma\Gamma}{2}\langle\delta\theta|L\delta\theta\rangle$$

$$= E(\theta(x)) + \frac{a\gamma\Gamma}{2}\sum_m \lambda_m\eta_m^2\,, \tag{3.4}$$

to second order of the perturbation $\delta\theta$. The change from $\delta\theta(x)$ to the η_m coordinates corresponds to a unitary transformation, therefore,

$$\frac{1}{a}\int(\delta\theta)^2 dx = \sum_m \eta_m^2\,. \tag{3.5}$$

Consider now a ring chain of length L (i.e., periodic boundary conditions). The spatially uniform states θ_s, θ_u generate the spatially uniform potential $R=1$ and $R=-1$, found by putting $\Delta\theta = 0$ and $\Delta\theta = \theta_u - \theta_s$, respectively, in Eq. (3.2b). Therefore, the perturbations can be assumed to have the form $\delta\theta(x,t) = \delta\theta_{q_m\omega}\exp i(q_m x - \omega t)$. With $q_m = (2\pi/L)m$, we find using Eqs. (3.1) and (3.2),

$$\lambda_m^s = \Gamma + (\kappa/\gamma)(2\pi/L)^2 m^2\,, \tag{3.6}$$

for the state θ_s and

$$\lambda_m^u = -\Gamma + (\kappa/\gamma)(2\pi/L)^2 m^2\,, \tag{3.7}$$

for the state θ_u. The state θ_s is, therefore, stable against small perturbations. The long wavelength perturbations decay with relaxation rate $\Gamma \geq 0$. Note, that Γ tends to zero as F approaches V_0 and the system exhibits a soft mode at $F = V_0$.[18] At this field the local extrema of the potential V, Eq. (2.3), vanish. The state θ_u, in contrast, is unstable against long wavelength modes $q_m < \xi^{-1}$.

Now consider the critical nucleus $\theta_N(x)$. In the case of the SAN [see Eq. (2.14)] we have to expand R formally in $\Delta\theta$, to linear order (to find the solution, we originally had to expand to second order in $\Delta\theta$). This leads to the eigenvalue problem

$$\left[-\xi^2\frac{d^2}{dx^2} + \left(1 - \frac{3}{\cosh^2(x/2\xi)}\right)\right]\delta\theta_\lambda = \left(\frac{\lambda}{\Gamma}\right)\delta\theta_\lambda\,. \tag{3.8}$$

Exactly the same eigenvalue problem has been found in the study of the stability of dipole domains in a bulk semiconductor current instability.[19] One finds localized modes for $\lambda_0^N = -5/4\Gamma$, $\lambda_1^N = 0$ and $\lambda_2^N = 3/4\Gamma$, and nonlocalized eigenfunctions for $\lambda \geq \Gamma$. The eigenvalue $\lambda = 0$ corresponds to the mode $\delta\theta_{N,1} = [\partial\theta_N(x+x_0)/\partial x_0]_{x_0=0}$, which restores the broken translational symmetry (Goldstone mode). The eigenmodes are discussed in Appendix A.

To find the spectrum of the critical nucleus over the whole range of F, we have evaluated the spectrum of $L(\theta_N(x))$ numerically. The result is shown in Fig. 5. At equilibrium $F=0$, the spectrum is that of two kinks infinitely apart, the eigenvalues show a twofold degeneracy. The solution θ_N corresponds to a saddle in the energy surface. The energy decreases in the direction of the unstable localized eigenmode $\delta\theta_{N,0}$ with a curvature $a\gamma/2\lambda_0^N < 0$ and increases in the direction of $\delta\theta_{N,n}$, $n \geq 2$ with curvatures $a\gamma/2\lambda_n^N$ determining the width of the pass at the saddle. In the direction $\delta\theta_{N,1}$ the saddle is flat. Note that the saddle becomes very flat in the direction $\delta\theta_{N,0}$ both for small fields and for F close to V_0, respectively. In these limits λ_0^N tends to zero.

The amplitude η_0 of the unstable mode $\lambda_0^N < 0$ describes the expansion or contraction of the nucleus. The critical nucleus can be regarded as

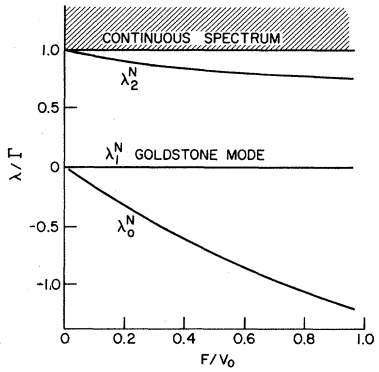

FIG. 5. Eigenvalues of the perturbations of the critical nucleus. In the whole field range $0 < F < V_0$ we find three localized modes; an unstable mode with eigenvalue $\lambda_0 < 0$ corresponding to expansion or contraction of the nucleus, a translation mode with eigenvalue $\lambda = 0$, and a localized mode λ_2^N. For $\lambda \geq \Gamma$ the eigenmodes of the nucleus are nonlocalized. The curves shown are universal. $\Gamma = (V_0/\gamma)[1-(F/V_0)^2]^{1/2}$.

a kink-antikink pair separated by a distance d_{crit}. A positive value for η_0 pushes the kink-antikink pair farther apart, and a negative value brings the pair closer together. If the separation d of the pair is large, then the driving force will supply an energy $-F\Delta d$ through an increase in their separation by Δd. Figure 6 shows a qualitative sketch of the energy $\Delta E(d)$ associated with a kink-antikink pair. After the kink and antikink move away from each other they will eventually recombine with other kinks. The location of the recombination events depends not only on the separation of the original pair but also on the coordinates of the other kinks involved in the recombination.

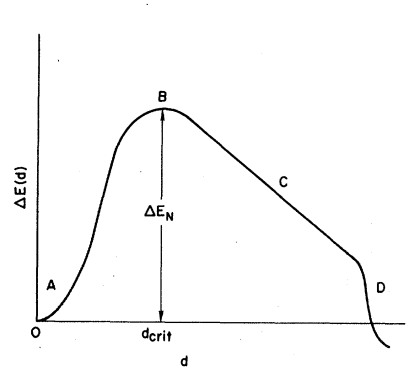

FIG. 6. Qualitative sketch of the energy of a kink-antikink pair separated by a distance d. In the Peirls valley (A) the chain is uniform. Energy must be supplied to pull the kink and antikink apart until a critical separation d_{crit} is reached given by the width of the critical nucleus (B). In the range (C) the energy change is dominated by the applied force, rather than by interaction of the original partners. At D recombination with another kink terminates the motion of one of the original partners.

IV. THE BLSL APPROACH

In this section we will derive an expression for the nucleation rate using the BLSL approach.[5-7] Equations (1.1) and (1.2) are equivalent to the (functional) Fokker-Planck equation

$$\frac{\partial P}{\partial t}+\frac{1}{a}\int dx\,\frac{\delta j(\theta)}{\delta\theta}=0\,, \tag{4.1}$$

where

$$j(\theta)=-\frac{1}{\gamma a}\left(\frac{\delta E}{\delta\theta}P+kT\frac{\delta P}{\delta\theta}\right) \tag{4.2}$$

is the probability current, and $P(\theta(x))$ is the probability distribution.

At low temperatures large segments of the chain lie in the local minima (Peierls valley) of the potential V, Eq. (2.3), i.e., at $d=0$ in Fig. 6. The original BLSL derivations point out that for $\Delta E_N \gg kT$, we can expect serious departures from equilibrium to occur only in the vicinity of the saddle point. Thus $P(\theta)$ has the form of an equilibrium distribution, within a single Peierls valley. It is taken to be normalized so that[5-7]

$$\int_{\text{valley}} P(\theta(x))D\theta(x)\approx 1\,, \tag{4.3}$$

where $D\theta(x)$ denotes a functional integration. The equilibrium distribution is given by $P(\theta)=\mathfrak{N}\times\exp[-E(\theta)/kT]$, where $E(\theta)$ is given by Eq. (2.1) and $\mathfrak{N}$ is a normalization factor. Using the quadratic approximation, Eq. (3.4), near $\theta(x)=\theta_s$, we find for the local equilibrium distribution

$$P_{\text{loc}}(\{\eta\})=\frac{1}{Z_s}\exp\left(-\frac{a\gamma}{2kT}\sum_n \lambda_n^s\eta_n^2\right), \tag{4.4}$$

which upon normalization according to Eq. (4.3) yields

$$\frac{1}{Z_s^2}=\prod_n\left(\frac{a\gamma\lambda_n^s}{2\pi kT}\right). \tag{4.5}$$

The BLSL approach makes the following ansatz for the distribution function:

$$P(\theta(x))=\beta(\theta(x))\exp\left(-\frac{E(\theta)}{kT}\right), \tag{4.6}$$

where $\beta(\theta(x))$ is a correction to the local equilibrium distribution. As a result of Eqs. (4.3) and (4.4) $\beta(\theta(x))$ must, near θ_s, be given by

$$\beta(\theta_s)=\frac{1}{Z_s}\exp\left(\frac{E(\theta_s)}{kT}\right), \tag{4.7}$$

i.e., be independent of $\theta(x)$. Elsewhere $\beta(\theta(x))$ is found in the following way.[5-7] We introduce the ansatz (4.6) into (4.4) and find that the current is

$$j(\theta)=-\frac{kT}{\gamma a}\left(\frac{\delta\beta}{\delta\theta}\right)\exp\left(-\frac{E(\theta)}{kT}\right). \tag{4.8}$$

Now consider (4.8) at the saddle. We obtain

$$j_n(\{\eta\}) = -\frac{kT}{\gamma a}\frac{\partial\beta(\{\eta\})}{\partial\eta_n}\exp\left(-\frac{E_N}{kT}-\frac{a\gamma}{2kT}\sum_n \lambda_n^N\eta_n^2\right), \tag{4.9}$$

using the coordinate system given by the unitary transformation of Eq. (3.3). To find the stationary distribution, Eq. (4.16), we must require that the divergence of the current vanishes

$$\sum_n \frac{\partial}{\partial\eta_n} j_n(\{\eta\}) = 0 . \tag{4.10}$$

The only nonvanishing current component is the flow across the saddle; $j_0(\{\eta\}) \neq 0$ and $j_n(\{\eta\}) = 0$, $n > 0$. Integration of (4.9) for $n = 0$ yields

$$\beta(\{\eta\}) = -\frac{\gamma a}{kT}\int d\eta_0 j_0(\{\eta\})\exp\left(\frac{E_N}{kT}+\frac{a\gamma}{2kT}\sum_n \lambda_n^N\eta_n^2\right). \tag{4.11}$$

Because $j_n(\{\eta\}) = 0$ for $n > 0$, $\beta(\{\eta\})$ must, according to Eqs. (4.9) and (4.10), be a function of η_0 alone. This is only the case if

$$j_0(\{\eta\}) = I\exp\left(-\frac{a\gamma}{2kT}\sum_{n>0}\lambda_n^N\eta_n^2\right), \tag{4.12}$$

where I is a constant, which depends on the boundary conditions imposed on $\beta(\eta_0)$, far from the saddle point.

In the literature of the thermally activated barrier crossing[3,5-7] it is assumed that the local equilibrium distributions, on their respective sides of the saddle point, are connected by the diffusively driven flux Eq. (4.12) over the saddle point. In our situation, we must, however, remember that the crossing of the saddle point represents generation of a kink-antikink pair under the action of an external force. If the applied field is strong, the kink and antikink are immediately driven apart, and the chain configuration is driven away from the saddle. The kink and antikink have a negligible chance of returning to their original partners and recombining with these. Thus, in our case, the diffusion over the saddle point in the direction of positive η_0 ($d > d_{\text{crit}}$ in Fig. 6) connects us to a sink. We can, therefore, treat the diffusion over the saddle as if the distribution function vanishes in the region of positive η_0, i.e., in the region of separated kink-antikink pairs. Thus, we will require that $\beta(+\infty) = 0$. In the direction of subcritical separation (i.e., negative η_0) the normal BLSL picture applies. The distribution function will increase rapidly as we go toward negative η_0, to the local equilibrium value Eq. (4.7). Thus $\beta(-\infty)$ is given by Eq. (4.7). Integration of Eqs. (4.11) and (4.12) over $d\eta_0$ with these boundary conditions yields

$$I = \frac{kT}{\gamma a}\left(\frac{\gamma a|\lambda_0^N|}{2\pi kT}\right)^{1/2}\frac{1}{Z_s}\exp\left(-\frac{\Delta E_N}{kT}\right), \tag{4.13}$$

where $\Delta E_N = E_N - E_s$ is the activation energy barrier discussed in Sec. II and shown in Fig. 4.

The total current across the saddle is found by integrating (4.12) over all coordinates perpendicular to η_0. Special attention has to be given to the Goldstone mode coordinate η_1. The integral $d\eta_1$ can be transformed into an integral over ds, the effective lateral displacement of the nucleus.[7] We have, according to Eq. (3.5),

$$d\eta_1^2 = \frac{1}{a}\int(\delta\theta_{\lambda=0})^2 dx , \tag{4.14}$$

but $\delta\theta_{\lambda=0} = (d\theta_N(x+s)/ds\,|_{s=0})ds$ and therefore,

$$\int d\eta_1 = \int_0^L\left[\frac{1}{a}\int\left(\frac{d\theta_N}{dx}\right)^2 dx\right]^{1/2} ds = L\left(\frac{\Delta E_N}{\kappa a}\right)^{1/2}, \tag{4.15}$$

where L is the length of the chain. In Eq. (4.15), we have made use of Eq. (2.11). Thus, we find after integration of Eq. (4.12) over all perpendicular coordinates a total current per unit length of the chain

$$j = \frac{kT}{\gamma a}\left(\frac{\Delta E_N}{\kappa a}\right)^{1/2}\left(\frac{\gamma a|\lambda_0^N|}{2\pi kT}\right)\left(\frac{Z_N}{Z_s}\right)\exp\left(-\frac{\Delta E_N}{kT}\right), \tag{4.16}$$

where Z_N is given by

$$\frac{1}{Z_N^2} = \prod_{n\neq 1}\left(\frac{a\gamma|\lambda_n^N|}{2\pi kT}\right). \tag{4.17}$$

Substituting the explicit expressions for Z_N and Z_s, we obtain

$$j = \frac{1}{(2\pi)^{3/2}}\left(\frac{\gamma}{\kappa}\right)^{1/2}(|\lambda_0^N|Q)\left(\frac{\Delta E_N}{kT}\right)^{1/2}\exp\left(-\frac{\Delta E_N}{kT}\right), \tag{4.18}$$

where

$$Q^2 = \left[\frac{\lambda_0^s}{|\lambda_0^N|}\lambda_1^s\frac{\lambda_2^s}{\lambda_2^N}\prod_{m=3}^{\infty}\frac{\lambda_m^s}{\lambda_m^N}\right]. \tag{4.19}$$

All quantities, except Q have been determined in Secs. II and III. In the SAN case Q can be evaluated analytically. Using techniques provided by Langer[20] and McCumber and Halperin,[17] we find $Q^2 = 60\Gamma$ [see Appendix B, Eq. (B9)]. In the case of the SAN, we thus find

$$j = \frac{1}{(2\pi)^{3/2}}\frac{5}{2}(15)^{1/2}\left(\frac{\gamma^{1/2}\Gamma^{3/2}}{\kappa^{1/2}}\right)\left(\frac{\Delta E_N}{kT}\right)^{1/2}\exp\left(-\frac{\Delta E_N}{kT}\right), \tag{4.20}$$

where ΔE_N is given by Eq. (2.19). For smaller fields, we have evaluated Q numerically as described in Appendix B.

Let us now discuss the range of validity of our

equations. To obtain Eq. (4.13), we required that fluctuations taking the chain past the saddle point result in kinks and antikinks moving rapidly away from each other. This will be the case if the kink-antikink pair can gain an energy large compared to kT by moving away from each other. The total energy gained by a kink-antikink pair, through their separation is $2\pi lF$, where l is the distance moved before annihilation. This distance, in turn, is determined by the mean separation of kinks. Therefore, l is of the order of $1/m_0$, where m_0 is the density of kinks. Thus our approach will be valid for fields $F \gg m_0 kT$.

The BLSL approach requires, quite generally, that the activation energy barrier ΔE_N is large compared to kT. This limits the validity of our approach at large fields. We are, therefore, unable to describe the approach to the critical region[21] $F \cong V_0$, as can be done by the methods of Refs. 12 and 13.

V. FORCED STEADY MOTION OF THE CHAIN

Once a pair is created, the motion of its constituents, the kink and the antikink, is determined by the deterministic drift, and the fluctuations become unimportant. To investigate the motion of these driven kinks, we return, therefore, to the deterministic equation of motion Eq. (2.2). We search, quite generally, for traveling waves $\theta(z)$ which depend on x and t only in the combination $z = x + ut$, where u is the propagation velocity in the minus x direction. In a frame, moving with velocity u, Eq. (2.2) becomes

$$\gamma \frac{\partial \theta}{\partial \tau} + u\gamma \frac{\partial \theta}{\partial z} = -V_0 \sin\theta + F + \kappa \frac{\partial^2 \theta}{\partial z^2} . \tag{5.1}$$

The traveling waves are the stationary (time-independent) solutions of this equation. They are, therefore, found as solutions of

$$\kappa \frac{d^2\theta}{dz^2} - u\gamma \frac{d\theta}{dz} - V_0 \sin\theta + F = 0 , \tag{5.2}$$

which describes the motion of a particle with mass $m = \kappa$ in a potential $U = -V$ (Fig. 2), with damping $\eta = -u\gamma$, and with time t replacing the coordinate z. We need solutions $\theta_K(z)$ which describe a transition of the chain from one Peierls valley to an adjacent one [i.e., $\lim_{z\to+\infty}\theta_K(z) = \theta_s + 2\pi$ and $\lim_{z\to-\infty}\theta_K(z) = \theta_s$]. That means that for a given field F, a friction constant $\eta = \eta_c$ has to be found such that the corresponding dynamical system, Eq. (5.2), possesses a solution of the following type: A particle starting at $t \to -\infty$ from θ_s (a local maximum of U, see Fig. 2) settles at $t \to +\infty$ at an adjacent peak of U, which is $2\pi F$ lower. If the friction constant η is too high a particle starting at θ_s will simply settle into the next local minimum of the potential U (at $\theta_u - 2\pi$). If the friction η is too low then the particle gains enough kinetic energy to overrun the next potential hill and all the following hills.

We have determined η_c numerically by this procedure; for a given field F and friction η, we start a particle at $t = -\infty$ on a potential hill of U at θ_s. If the particle settles in the adjacent minimum we have found an upper bound for η_c, if it arrives on the next potential hill (with nonzero velocity) we have found a lower bound of η_c. By varying η in small steps, η_c can be determined accurately. We then repeat this calculation for different values of the field to find η_c as a function of F. The propagation velocity[2,22] $u(F) = -\eta_c(F)/\gamma$ is shown in Fig. 7. For small fields u is linear in F and it increases monotonically to a value $u^*/u_0 \cong 1.19$ at $F = V_0$ in accordance with Ref. 23. For damping coefficients larger than $\eta^* = -1.19 u_0 \gamma$ the motion of the particle with mass $m = \kappa$, Eq. (5.2), is overdamped. For $F = V_0$ there is a kink for every propagation velocity $u > u^*$. The limiting kink[18] with $u = \infty$ shows no spatial variation and corresponds to advancement by 2π of the uniform chain.

The low field mobility of the kinks can be calculated analytically. Consider the single-particle equivalent equation of motion Eq. (5.2). When the particle travels from one peak of U (at θ_s) to an adjacent one (at $\theta_s + 2\pi$) it loses the potential energy $2\pi F$. Because the particle is at rest at the two peaks, the energy loss $2\pi F$ must be accounted for by the damping. In the low friction limit[24] ($u \to 0$) the energy loss can be calculated from $\int \eta \dot{\theta} d\theta$, where both the limits and the function $\dot{\theta}(t)$ describe the undamped motion for $\eta = F = 0$,

$$2\pi F = -\int_0^{2\pi} \eta \dot{\theta} d\theta . \tag{5.3}$$

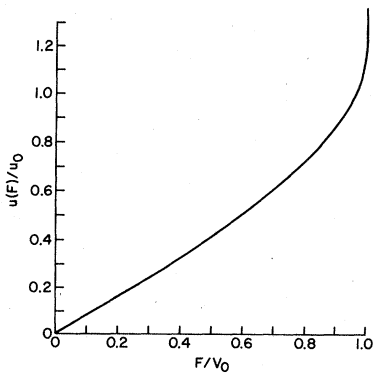

FIG. 7. Propagation velocity of a kink as a function of the field. In the variables u/u_0, F/V_0 the curve shown is universal. $u_0 = (\kappa V_0)^{1/2}/\gamma$.

With the velocity $\dot{\theta}=(2V_0/m)^{1/2}(1-\cos\theta)^{1/2}$ of the undamped particle at $F=0$ we find[2,25]

$$\mu=u/F=\frac{\pi}{4\gamma}\left(\frac{\kappa}{V_0}\right)^{1/2}. \tag{5.4}$$

Next, we will investigate the stability of the driven kinks. We add small perturbations $\delta\theta(z,\tau)$ to the kink solution θ_K. Linearizing Eq. (5.1) with respect to $\delta\theta(z,\tau)$ yields a time-evolution equation for the perturbations

$$\gamma\frac{\partial\delta\theta(z,\tau)}{\partial\tau}+\gamma u\frac{\partial\delta\theta(z,\tau)}{\partial z}=-V_0\cos\theta_K\delta\theta(z,\tau)+\kappa\frac{\partial^2\delta\theta(z,\tau)}{\partial z^2}. \tag{5.5}$$

Because the kink is stationary in the moving frame the perturbations have the form $\delta\theta(z,\tau)=\delta\theta_\lambda(z)\times\exp(-\lambda\tau)$. The stability of the kink $\theta_K(z)$ is, therefore, determined by the eigenvalue problem

$$\left(-\kappa\frac{d^2}{dz^2}+\gamma u\frac{d}{dz}+V_0\cos\theta_K(z)\right)\delta\theta_\lambda(z)=\gamma\lambda\delta\theta_\lambda(z). \tag{5.6}$$

This eigenvalue problem is not Hermitian. The localized eigenmodes which are carried along with the driven kink can, however, be found as solutions of a Hermitian eigenvalue problem. With the transformation $\delta\theta_\lambda(z)=e^{+(u\gamma/2\kappa)z}\psi_\lambda(z)$, we find

$$\left(-\kappa\frac{d^2}{dz^2}+V_0\cos\theta_K(z)+\frac{1}{4}\frac{u^2\gamma^2}{\kappa}\right)\psi_\lambda(z)=\lambda\gamma\psi_\lambda(z). \tag{5.7}$$

Localized eigenfunctions of (5.7) are localized eigenfunctions of (5.6) as long as $\lambda<V_0/\gamma\cos\theta_s=\Gamma$. In this case the eigenfunctions of (5.7) decay as $\exp[-(\Gamma\gamma/\kappa+\frac{1}{4}u^2\gamma^2/\kappa^2-\lambda\gamma/\kappa)^{1/2}|z|]$ for $z\to\pm\infty$ and thus also $\delta\theta_\lambda(z)$ decays exponentially at large z. The lowest eigenmode of (5.7) is, however, the Goldstone mode $\psi_{\lambda=0}(z)=e^{-(u\gamma/2\kappa)z}[d\theta_K(z+z_0)/dz_0]_{z_0=0}$, with eigenvalue $\lambda=0$. Hence all localized eigenfunctions have eigenvalues $\lambda\geq 0$ and all nonlocalized eigenfunctions have, for $F<V_0$, eigenvalues with $\mathrm{Re}\lambda\geq V_0\cos\theta_s/\gamma=\Gamma\geq 0$. For $F<V_0$ this proves that the driven kinks are stable against small perturbations.

We now have all the information that is needed to calculate the average displacement change $\langle\partial\theta/\partial t\rangle$ of a chain in the presence of a field F. On a long term scale the advance of $\theta(x,t)$ at some point x is given by the numbers of kinks and antikinks which pass this point (see Fig. 1). A kink passing the point x to the right reduces θ by 2π and an antikink passing x to the right advances θ by 2π. In the presence of a field, we have a kink current $J_K=-um$ and an antikink current $J_{AK}=un$, where m is the kink density and n is the antikink density, respectively. Therefore,

$$\langle\partial\theta/\partial t\rangle=-2\pi(\langle J_K\rangle-\langle J_{AK}\rangle)=4\pi un_0, \tag{5.8}$$

where $n_0=\langle n\rangle=\langle m\rangle$ is the average kink (antikink) density in a ring chain.

A steady-state density $2n_0$ is maintained by a balance of the annihilation (recombination) and the nucleation of kink-antikink pairs. The recombination rate can be found by the argument that follows. The probability that a kink encounters an antikink in the time interval dt is given by the probability that there is an antikink in the range $2udt$ swept out by the relative motion within that time. Since the density of antikinks is n, the probability is $2undt$. The rate of recombination of m kinks per unit length and time is, therefore, $2unm$. The balance for the steady-state densities becomes

$$j-2un_0^2=0, \tag{5.9}$$

where j is the nucleation rate derived in the previous section.

In this consideration, we have again neglected the diffusive motion of the kinks. This is a good approximation as long as the distance l_D a kink would diffuse during its lifetime $\tau=(2um_0)^{-1}$, is much smaller than the distance $l_u=u\tau=(2m_0)^{-1}$ it travels during this same time τ. With the diffusion constant $D=(\mu/2\pi)kT$ of the kinks,[26] we find $l_D=(2D\tau)^{1/2}$. In the ohmic limit, $u=\mu F$ and the ratio $l_D/l_u=(2m_0kT/\pi F)^{1/2}$ is small, if $F\gg 2m_0kT/\pi$. This is the same condition which we imposed on (4.13) and hence on (4.18). Thus (5.9) is valid for $F\gg 2m_0kT/\pi$.

The statistical properties of the kink gas have been investigated from a more microscopic viewpoint in Ref. 27. There it is shown that (5.9) is valid when $(jL^x/2u)\gg 1$, i.e., in the thermodynamic limit considered here. Note also that Eq. (5.9) predicts a steady-state density n_0 which is independent of the damping coefficient γ. Both the nucleation current j and the propagation velocity u of the kinks are proportional to γ^{-1}. When we measure j in units $j_0=(V_0/\kappa)^{1/2}(V_0/\gamma)$ then j/j_0 depends only on $\tau=kT/(\kappa V_0)^{1/2}$ and F/V_0. If u is measured in units of $u_0=(\kappa V_0)^{1/2}/\gamma$ then u depends only on F/V_0. Hence, according to Eq. (5.9), n_0 is proportional to $(j_0/2u_0)^{1/2}=(V_0/\kappa)^{1/2}$ and depends only on the scaled temperature τ and the scaled field F/V_0. Indeed, the steady-state density n_0 must be independent of γ because the stationary distribution of the functional Fokker-Planck equation, Eqs. (4.1) and (4.2), is independent of γ. This is the case in the heavy damping limit only. Thus a γ independent steady-state density of kinks characterizes the heavy damping limit.

With (5.9) the average angular particle velocity becomes

$$\left\langle \frac{\partial\theta}{\partial t} \right\rangle = 2\pi(2uj)^{1/2} . \tag{5.10}$$

The result for the SAN case based on Eqs. (5.10) and (4.20) is plotted in Fig. 8(a) and the numerical results for lower fields, based on Eqs. (5.10), (4.18), and (4.19), are shown in Fig. 8(b). In the variables $\langle\dot{\theta}\rangle\gamma/V_0$ the curves shown in Fig. 8 depend only on $\tau = kT/(V_0\kappa)^{1/2}$ and F/V_0, i.e., for a fixed τ and F/V_0 the mean angular velocity is proportional to γ^{-1} and increases with increasing amplitude of the sinusoidal potential V_0. Our results will be compared to earlier work in the next section.

VI. DISCUSSION

Our aim was the calculation of the nucleation rate j of kink-antikink pairs given by Eqs. (4.18)–(4.20). The motion of the kinks in presence of a field is determined by the propagation velocity $u(F)$ shown in Fig. 7. We have shown that the two parameters j and u determine the average angular velocity of the chain. Reference 27 demonstrates also that the long term dynamical behavior of the overdamped driven chain can be expressed as a function solely of j and u, without additional use of the other parameters of Eq. (1.1). Similar considerations show that the long term dynamical behavior of the overdamped chain at equilibrium is also determined by only two parameters, i.e., the diffusion constant (mobility) of the kinks and the equilibrium kink density.[26]

The average angular velocity of the chain has also been calculated via a transfer-operator technique[10,11] and a BBGKY hierarchy approximation.[12-14] In this work the ansatz

$$P(\{\theta_i\}) = P_{eq}(\{\theta_i\})h(\{\theta_i\}) , \tag{6.1}$$

is introduced in the Fokker-Planck equation

$$\frac{\partial P}{\partial t} = -\mathrm{div} j , \quad j = vP - D\nabla P . \tag{6.2}$$

Here, $v = -(1/\gamma)\nabla E$ is the many-dimensional velocity vector, $E = a[\sum V_0(1-\cos\theta_i) - F\theta_i + (\kappa/2a^2) \times (\theta_i - \theta_{i+1})^2]$ is the potential energy of the discrete chain, and i is the particle number. In Eq. (6.1) P_{eq} is the equilibrium distribution at $F=0$ and $h(\{\theta_i\})$ accounts for the corrections required by the fact that for $F>0$ the system is not in equilibrium and exhibits transport. The flux of probability, in terms of h, is given by

$$j = (F/\gamma)h(\{\theta_i\})P_{eq}(\{\theta_i\}) - D[\nabla h(\{\theta_i\})]P_{eq}(\{\theta_i\}) . \tag{6.3}$$

In the parts of configuration space where $P_{eq}(\{\theta_i\})$ is appreciable the first term on the rhs of Eq. (6.3) carries the current. Thus the kinks represented by P_{eq} can provide current flow via this first term; but where P_{eq} is small and current has to be carried, the second term must do it.

In a BBGKY hierarchy the n particle distribution function $h_n(\theta_1, \theta_2, \ldots, \theta_n)$ is expressed in terms of the $n+1, n+2, \ldots$, particle distribution function. In order to solve the problem Refs. 12–14 reduce the series of equations to an effective single particle problem, i.e., their correction factor h takes the form

$$h(\theta_1, \ldots, \theta_N) = h_s(\theta_1)h_s(\theta_2)\cdots h_s(\theta_N) . \tag{6.4}$$

Can this reduced ansatz provide the correct result? We have pointed out that nucleation is an essential step in the sequence, hence current must be carried over the saddle point. P_{eq} is small near the saddle, so ∇h has to be large. This can, however, not be achieved with (6.4), because the derivative of the correction factor has to be large along the saddle-point configuration $\theta_N(x)$, i.e., $\nabla h\,|_{\theta=\theta_N(x)}$ has to be large. With (6.4) the derivative of h can only be large for configurations which put many particles at the value of θ

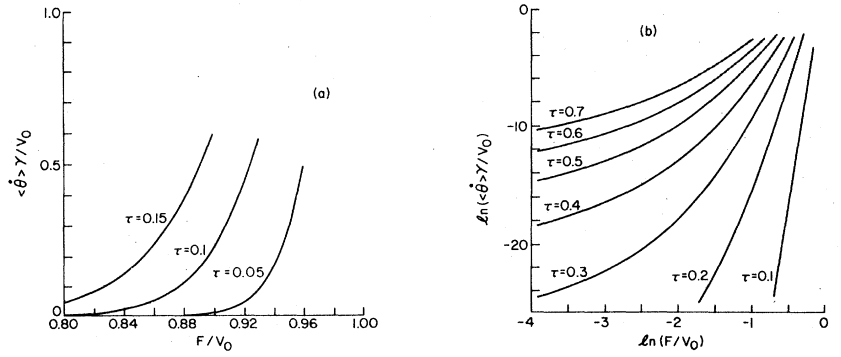

FIG. 8. Average particle velocity as a function of the applied force and scaled temperature $\tau = kT/(\kappa V_0)^{1/2} = 8kT/E_0$. The curves shown are universal. (a) SAN results and (b) computational results for smaller values of F.

where $\partial h_s(\theta_i)/\partial\theta_i$ is large. At small fields, however, to take one limit as an example, the saddle-point configuration has most of its particles near θ_s and near $\theta_s+2\pi$. $\partial h_s/\partial\theta_i$ cannot be large there, otherwise we get far too much flux in the vicinity of the spatially uniform states θ_s, $\theta_s+2\pi,\ldots,$. If, instead, we try to make $\partial h/\partial\theta_i$ large at $\theta_i=\theta_u$, i.e., at the maximum of the potential V [Eq. (2.3)], then the saddle-point configuration is not particularly favored compared, for example, to one which places more particles at θ_u. An example of such a fluctuation would be one in which the chain departs from θ_s, over a limited range, as in the case of the critical nucleus, but reaches its maximum deviation from θ_s near θ_u. Near equilibrium, Eq. (6.1) together with a constant h in Eq. (6.4), correctly describe the density of solitons. With increasing field the density of solitons increases. Once again the uncorrelated correction factors of Eq. (6.4) cannot describe this increase; a kink after all is a very specific spatial configuration and not just an increase in the relative number of particles for some ranges of θ. We also would like to point out that the treatment of Ref. 12–14 only requires that the divergence of the single-particle probability flux with components $J_1=\int d\theta_2\cdots d\theta_N j_1$ vanishes. Clearly $\mathrm{div}J=0$ is a necessary condition but not a sufficient one to yield $\mathrm{div}j=0$.

At small fields Refs. 12–14 find an angular velocity

$$\left\langle\frac{\partial\theta}{\partial t}\right\rangle\left(\frac{\gamma}{V_0}\right)=\left[\sqrt{2}\,\pi^{3/2}\left(\frac{E_0}{kT}\right)^{3/2}\exp\left(-\frac{E_0}{kT}\right)\right]\left(\frac{F}{V_0}\right). \quad (6.5)$$

Our own theory of Secs. IV and V does not apply to the low field limit. However, we can easily find the current in this limit. Near equilibrium for small fields Eq. (5.8) becomes

$$\left\langle\frac{\partial\theta}{\partial t}\right\rangle=2\pi\mu F(2n_{\mathrm{eq}}), \quad (6.6)$$

where μ is the zero field mobility given by Eq. (5.4) and $2n_{\mathrm{eq}}$ is the total equilibrium soliton density derived in Appendix C. We obtain

$$\left\langle\frac{\partial\theta}{\partial t}\right\rangle=2\pi\mu F\left(\frac{8}{\pi}\right)^{1/2}\left(\frac{V_0}{\kappa}\right)^{1/2}\left(\frac{E_0}{kT}\right)^{1/2}\exp\left(-\frac{E_0}{kT}\right), \quad (6.7)$$

which in the units of Fig. 7 becomes

$$\left\langle\frac{\partial\theta}{\partial t}\right\rangle\left(\frac{\gamma}{V_0}\right)=\left[\sqrt{2}\,\pi^{3/2}\left(\frac{E_0}{kT}\right)^{1/2}\exp\left(-\frac{E_0}{kT}\right)\right]\left(\frac{F}{V_0}\right), \quad (6.8)$$

and thus, for a given field F/V_0, depends only on the temperature measured in units of $(\kappa V_0)^{1/2}\propto E_0$. The rhs of Eq. (6.5) has an extra preexponential factor E_0/kT not contained in Eq. (6.8). A mobility can be found by comparing Eq. (6.5) with (6.7), yielding $\mu_{\mathrm{BBGKY}}=\mu(E_0/kT)$ which diverges as $T\to 0$.

A computer simulation[15] by Schneider and Stoll is best fit by a preexponential factor $(E_0/kT)^2$. However, the sample modeled by these authors shows only a few activated kinks. The angular chain velocity depends on the passage of the kinks past some point x, along the chain, as given by Eq. (5.8). In order to obtain reliable results for the thermodynamic limit, one has to model much larger systems containing many activated kinks over times which are large compared to the characteristic times of the soliton gas.[26,27] Therefore, a study of such a short sample[27] cannot easily be compared with Eqs. (6.5) or (6.8), attempting to describe the thermodynamic limit.

A comparison of our results over the whole range of fields shows that at low fields, the effective single-particle approach[12–14] overestimates the current as a result of the additional factor E_0/kT. At larger fields we can directly compare the activation energies. The effective single-particle activation energy shown in Fig. 10 of Ref. 13, is higher than the activation energy which we find (Fig. 4). Thus at higher fields our current will be larger than the one calculated via the BBGKY hierarchy. Comparing their result at $\tau\cong 0.63$ (their lowest temperature) with our result for $\tau=0.6$ we find a higher angular velocity for fields larger than $0.1V_0$. Whereas our approach is valid at low temperatures and strong coupling between adjacent pendulums the BBGKY approach will, of course, yield correct results in the high-temperature regime and weak-coupling limit when correlations between neighboring particles become unimportant. In that case, the many-particle system behaves much like the one-particle system.

Note added in proof. H. Thomas, in correspondence, has pointed out that Eq. (2.23) can be improved by matching the solution Eq. (2.17) to the kink solution Eq. (2.15). We obtain

$$\Delta E_N(F)=2E_0\left(1+\frac{\pi}{8}\left(\frac{F}{V_0}\right)\log\left(\frac{4\pi F}{64V_0}\right)\right)$$

for the activation energy at low fields.

APPENDIX A: EIGENFUNCTIONS OF THE SAN

Following Landau and Lifshitz[28] and Morse and Feshbach,[29] we can find the eigenfunctions of the eigenvalue problem for the SAN [Eq. (3.8)]. The unstable mode

$$\delta\theta_{N,0}(x)=\left[\tfrac{32}{15}(\xi/a)\right]^{1/2}\mathrm{sech}^3(x/2\xi), \quad (A1)$$

with eigenvalue $\lambda_0=-5/4\Gamma$ describes the contraction and expansion of the nucleus (separation of the kink-antikink pair). The exponential decay length ξ is given by Eq. (2.10) and Γ has been defined after Eq. (3.2). The second eigenmode has eigen-

value $\lambda_1 = 0$ and describes the translation (Goldstone mode) of the nucleus

$$\delta\theta_{N,1}(x) = [\tfrac{8}{15}(\xi/a)]^{1/2}\frac{\sinh(x/2\xi)}{\cosh^2(x/2\xi)}, \tag{A2}$$

and is the normalized derivative of the solution θ_N. In addition, we have a localized mode at $\lambda_2 = \frac{3}{4}\Gamma$ given by

$$\delta\theta_{N,2}(x) = [\tfrac{1}{24}(\xi/a)]^{1/2}\frac{1-4\sinh^2(x/2\xi)}{\cosh^3(x/2\xi)}, \tag{A3}$$

which describes the extension or contraction of the width of the kink and antikink bound in the nucleus. The scattering states $\lambda_q \geq \Gamma$ are

$$\delta\theta_{N,q}(x) = A(q)e^{iqx}[4ik + ik^3 - (9+6k^2)\tanh(x/2\xi) - 15ik\tanh^2(x/2\xi) + 15\tanh^3(x/2\xi)], \tag{A4}$$

where $k = 2q\xi$ and $A(q)$ is a normalization factor. This yields for the difference in density of states[30] between the nucleus θ_N and the uniform state θ_s:

$$\Delta\rho(k) = 3\delta(k) - \frac{6}{\pi}\frac{(11+8k^2+k^4)}{(36+49k^2+14k^4+k^6)}. \tag{A5}$$

APPENDIX B: DENSITY OF STATES

In this section, we will calculate the product of the eigenvalues Eq. (4.19). In the SAN limit as well as at equilibrium, we will use a method given by McCumber and Halperin.[17] We will adopt the notation of Ref. 17 and refer to this paper for a more detailed description of the method. In the SAN case, Eqs. (2.14) and (3.8), and for the equilibrium kink Eq. (2.15), the eigenvalue problem, Eq. (3.1), is of the form

$$\left(\frac{d^2}{dy^2} - 2\alpha(\epsilon^N) + 2\beta\,\mathrm{sech}^2 y\right)\psi_\epsilon^N(y) = 0 \tag{B1}$$

for the nonuniform states and

$$\left(\frac{d^2}{dy^2} - 2\alpha(\epsilon^s)\right)\psi_\epsilon^s(y) = 0 \tag{B2}$$

for the uniform state θ_s. Here β is a parameter determining the strength of the potential and $\alpha(\epsilon)$ is a linear function of the eigenvalue ϵ. We will later specify these parameters for the SAN case, Eqs. (2.14) and (3.8), and for the equilibrium kink Eq. (2.15). For a finite chain of length L, we adopt antisymmetric boundary conditions

$$\psi\left(\frac{L}{2}\right) = \psi\left(-\frac{L}{2}\right), \quad \left.\frac{d\psi}{dy}\right|_{y=L/2} = -\left.\frac{d\psi}{dy}\right|_{y=-L/2}. \tag{B3}$$

McCumber and Halperin[17] found that the product of eigenvalues

$$Q^2 = \left(\prod_{n=0}^{\infty}\epsilon_n^s\right)\Big/\left(\prod_{n\neq GM}^{\infty}|\epsilon_n^N|\right), \tag{B4}$$

where the Goldstone mode (GM) is excluded, the limit $L\to\infty$ is given by

$$Q^2 = \lim_{\epsilon\to 0^+}\epsilon\,|r(\alpha,\beta)|. \tag{B5}$$

The function

$$r(\alpha,\beta) = \prod_{n=1}^{\infty}\frac{[n-1+(2\alpha)^{1/2}][n+(2\alpha)^{1/2}]}{[n-1+(2\alpha)^{1/2}][n+(2\alpha)^{1/2}]-2\beta}, \tag{B6}$$

depends only on the amplitude of the nonuniform potential and α.

In the SAN case, we find by comparing Eq. (B1) and Eq. (3.8),

$$\alpha = 2 + 2\lambda/\Gamma, \quad \beta = 6. \tag{B7}$$

Evaluation of the product in Eq. (B6) yields

$$r(\alpha,6) = -\frac{[1+(2\alpha)^{1/2}][2+(2\alpha)^{1/2}][3+(2\alpha)^{1/2}]}{[1-(2\alpha)^{1/2}][2-(2\alpha)^{1/2}][3-(2\alpha)^{1/2}]}. \tag{B8}$$

The function $r(\alpha,6)$ becomes $-60/(\lambda/\Gamma)$ in the limit $\lambda/\Gamma\to 0$. Hence in the SAN limit we find

$$Q^2 = 60\Gamma. \tag{B9}$$

The eigenvalues characterizing the perturbations of the equilibrium kink are determined by the Schrödinger equation

$$\left\{-\xi_0^2\frac{d^2}{dx^2} + \left[1 - 2\,\mathrm{sech}^2\left(\frac{x}{\xi_0}\right)\right]\right\}\psi_\lambda^K(x) = \frac{\lambda^K}{\Gamma}\psi_\lambda^K(x), \tag{B10}$$

obtained by evaluating (3.1) and (3.2) for $\Delta\theta(x)$ given by (2.15). Comparison with Eq. (B2) shows that in this case

$$\alpha = \frac{1}{2} + \frac{1}{2}\frac{\lambda}{\Gamma}, \quad \beta = 1. \tag{B11}$$

Evaluation of $r(\alpha,1)$ yields

$$r(\alpha,1) = -\frac{[1+(2\alpha)^{1/2}]}{[1-(2\alpha)^{1/2}]}, \tag{B12}$$

which approaches $4/(\lambda/\Gamma)$ as (λ/Γ) goes to zero. Hence at equilibrium

$$Q^2 = 4\Gamma. \tag{B13}$$

Outside these analytical limits, we proceed in the following way. We define

$$(\Delta Q)^2 = \left[\prod_{n=0}^{\infty}\left(\frac{\lambda_n^s}{\Gamma}\right)\right]\Big/\left[\prod_{n=3}^{\infty}\left(\frac{\lambda_n^N}{\Gamma}\right)\right], \tag{B14}$$

which is related to Q^2 by

$$Q^2 = \frac{\Gamma}{|\lambda_0^N|}\frac{\Gamma}{\lambda_1^N}(\Delta Q)^2\Gamma. \tag{B15}$$

Taking the logarithm of Eq. (B14) and introducing the density of states ρ_N for the nucleus and ρ_s for the uniform state, we find

$$\log(\Delta Q)^2 = \int_1^{\infty}(\rho_s - \rho_N)\log(\lambda/\Gamma)\,d(\lambda/\Gamma). \tag{B16}$$

To evaluate (B16), we have to calculate the density

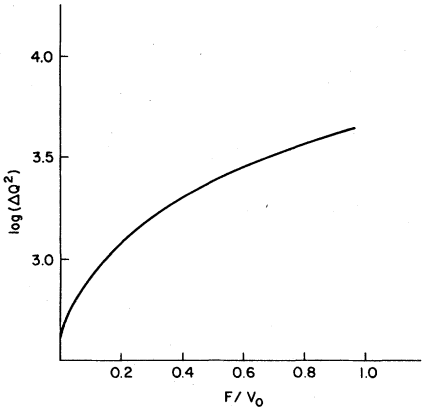

FIG. 9. Numerical evaluation of the product of the eigenvalues of the uniform state divided by the product of the eigenvalues of the nonlocalized eigenmodes of the critical nucleus.

of states ρ_N and ρ_s. We consider the Hamiltonian density

$$H=\xi^2\left(\frac{d\psi}{dx}\right)^2+R\psi^2\,, \tag{B17}$$

belonging to the Schrödinger operator L (Eq. 3.2) and apply the approximate quantization rule

$$\int p\,dx=2\pi\hbar n\,, \tag{B18}$$

where $p=\{2m[(\lambda/\Gamma)-R]\}^{1/2}$ and $m=\hbar^2/2\xi^2$. This yields a density of states for the critical nucleus, after differentiation with respect to (λ/Γ),

$$\rho_N=\frac{1}{2\pi\xi}\int\frac{dx}{[(\lambda/\Gamma)-R(\theta_N(x))]^{1/2}}\,, \tag{B19}$$

and for the uniform stationary state θ_s of a chain of length L

$$\rho_s=\frac{L}{2\pi\xi}\frac{1}{[(\lambda/\Gamma)-1]^{1/2}}\,, \tag{B20}$$

where we have used that $R(\theta_s)=1$. Two states belong to each eigenvalue of the continuous spectrum. We have evaluated the rhs of Eq. (B19) numerically. The result, Eq. (B16), is shown in Fig. 9. At low fields $(\Delta Q)^2$ must approach the result for a kink-antikink pair infinitely far apart. Through Eq. (B13) one finds $\log(\Delta Q)^2=2\log 4\cong 2.77$. For large fields $(\Delta Q)^2$ must approach the result for the SAN. From Eqs. (B9) and (B14) we find $\log(\Delta Q)^2=\log(\frac{3}{5}\,\frac{3}{4}\,60)=\log(56.25)\cong 4.03$. The results of Fig. 9 together with the eigenvalues of the localized eigenfunctions shown in Fig. 5 have been used to calculate the thermal activation rate j shown in Fig. 8(b).

The results in Eqs. (B9) and (B13) can also be obtained by invoking the density of states $\rho(q)$, calculating Q^2 via an equation similar to Eq. (B16) in q space. Here q is the wave vector of the nonlocalized eigenfunctions (see Eq. A4). In the SAN case, we use for the difference in density of states Eq. (A5). For the equilibrium kink the corresponding quantity is given in Ref. 30.

APPENDIX C: EQUILIBRIUM SOLITON DENSITY

We have shown that in linear response the mean angular particle velocity $\langle\partial\theta/\partial t\rangle$ is proportional to the equilibrium kink and antikink densities. Seeger and Schiller[1] find that the equilibrium density of kinks is given by the quotient of the partition function of a chain with a kink divided by the partition function of the kinkless chain. In our case, this quotient is given by

$$n_{eq}=\frac{1}{L}\frac{\int d\eta_0^K d\eta_1^K\cdots\exp\left(-\frac{\gamma a}{2kT}\sum\lambda_n^K(\eta_n^K)^2\right)}{\int d\eta_0^s d\eta_1^s\cdots\exp\left(-\frac{\gamma a}{2kT}\sum\lambda_n^s(\eta_n^s)^2\right)}\exp\left(-\frac{E_0}{kT}\right), \tag{C1}$$

where the λ_n^K are the eigenvalues of Eq. (B10), and λ_n^s are the eigenvalues of the kinkless chain. E_0 is the equilibrium kink energy Eq. (2.20). Integration over the η coordinates yields

$$n_{eq}=(1/L)(\gamma a/2\pi kT)^{1/2}Q\left(\int d\eta_0^K\right)\exp\left(-\frac{E_0}{kT}\right), \tag{C2}$$

where Q is given by Eq. (B13). The integral over the Goldstone mode coordinate yields [compare with Eq. (4.15)],

$$\int d\eta_0^K=(E_0/\kappa a)^{1/2}L\,, \tag{C3}$$

and, therefore, the equilibrium kink density becomes

$$n_{eq}=\left(\frac{2}{\pi}\right)^{1/2}\left(\frac{V_0}{\kappa}\right)^{1/2}\left(\frac{E_0}{kT}\right)^{1/2}\exp\left(-\frac{E_0}{kT}\right). \tag{C4}$$

The total soliton density (kinks and antikinks) in a chain with periodic boundary conditions is twice the kink density. Our derivation of the kink density Eq. (C4) differs from that of Seeger and Schiller only in the treatment of the translational degree of freedom of the kinks. The result Eq. (C4) agrees with that of Seeger and Schiller [Eq. (287) in Ref. 1] and also with the result given in Ref. 30 [Eq. (335) and Table I]. Agreement with the results derived from the transfer method hinges on the careful evaluation of the eigenvalues of the transfer operator.[31]

[1]A. Seeger and P. Schiller, in *Physical Acoustics, Vol. III*, edited by W. P. Mason (Academic, New York, 1966), p. 361.
[2]M. Büttiker and R. Landauer, Phys. Rev. Lett. 43, 1453 (1979).
[3]H. A. Kramers, Physica (Utrecht) 7, 284 (1940).
[4]G. H. Vineyard, J. Phys. Chem. Solids 3, 121 (1957).
[5]H. C. Brinkman, Physica (Utrecht) 12, 149 (1956).
[6]R. Landauer and J. A. Swanson, Phys. Rev. 121, 1668 (1961).
[7]J. S. Langer, Phys. Rev. Lett. 21, 973 (1968); Ann. Phys. (N.Y.) 54, 258 (1969).
[8]*Solitons and Condensed Matter Physics*, edited by A. R. Bishop and T. Schneider (Springer, Heidelberg, 1978).
[9]A. R. Bishop, J. A. Krumhansl, and S. E. Trullinger, Physica (Utrecht) 1D, 1 (1980).
[10]D. J. Scalapino, M. Sears, and R. A. Ferell, Phys. Rev. B 6, 3409 (1972).
[11]J. A. Krumhansl and J. R. Schrieffer, Phys. Rev. B 11, 3535 (1975).
[12]S. E. Trullinger, M. D. Miller, R. A. Guyer, A. R. Bishop, F. Palmer, and J. A. Krumhansl, Phys. Rev. Lett. 40, 406 (1978); 40, 1063(E), (1978).
[13]R. A. Guyer and M. D. Miller, Phys. Rev. A 17, 1774 (1978).
[14]K. C. Lee and S. E. Trullinger, Phys. Rev. B 21, 589 (1980).
[15]T. Schneider and E. Stoll, in Ref. 8, p. 326.
[16]J. S. Langer and V. Ambegaokar, Phys. Rev. 164, 498 (1967).
[17]D. E. McCumber and B. I. Halperin, Phys. Rev. B 1, 1054 (1970).
[18]M. Büttiker and H. Thomas, Phys. Lett. A 77, 372 (1980).
[19]M. Büttiker and H. Thomas, Phys. Rev. Lett. 38, 78 (1977); Z. Phys. B 34, 301 (1979).
[20]J. S. Langer, Ann. Phys. (N.Y.) 41, 108 (1967).
[21]T. Schneider, E. P. Stoll, and R. Morf, Phys. Rev. B 18, 1417 (1978).
[22]To obtain the correct $u(F)$ values from Ref. 2, one has to multiply $u(F)$ shown in Fig. 1 by $[1-(F/V_0)^2]^{1/2}$.
[23]M. Urabe, J. Sci. Hiroshima Univ. Ser. A 18, 379 (1955).
[24]R. Landauer, Phys. Rev. A 15, 2117 (1977).
[25]M. B. Fogel, S. E. Trullinger, A. R. Bishop, and J. A. Krumhansl, Phys. Rev. Lett. 36, 1411 (1976); Phys. Rev. B 15, 1578 (1977).
[26]M. Büttiker and R. Landauer, J. Phys. C 13, L325 (1980).
[27]C. H. Bennett, M. Büttiker, R. Landauer, and H. Thomas, J. Stat. Phys. 24, 421 (1981).
[28]D. L. Landau and E. M. Lifshitz, *Quantum Mechanics* (Addison-Wesley, Reading, Mass., 1958), p. 69. problem 4.
[29]P. M. Morse and H. Feshbach, *Methods of Theoretical Physics* (McGraw-Hill, New York, 1953), Vol. II, p. 1650.
[30]J. F. Currie, J. A. Krumhansl, A. R. Bishop, and S. E. Trullinger, Phys. Rev. B 22, 477 (1980).
[31]R. M. Leonardis and S. E. Trullinger, Phys. Rev. A 20, 2603 (1979).